Patryk Radziszewski, Maksymilian Cierniewski, Karol Bryk

Analysis of the Energy Consumption of a Rail Passenger Vehicle Powered by a Hydrogen Fuel Cell

Abstract: The article presents a proposal for the installation of components of a hydrogen power supply system in a rail passenger vehicle. The research work discussed in the article involved the analysis of various vehicle configurations and the determination of traction characteristics, which, subsequently, were used to perform a series of theoretical simulations of journeys on a specific route in relation to various assumptions. The tests led to the calculation of average energy consumption and the assessment of hydrogen consumption for a selected vehicle configuration.

Key words: hydrogen fuel cell, electric multiple unit, traction battery, emission-free drive system

DOI: 10.32730/mswt.2024.68.6.8

1. Introduction

Electric multiple units constitute the basis of regional passenger transport. They provide cheap passenger transport on electrified routes (diesel multiple units being used on other routes). In order to protect the environment, it is possible to replace the aforesaid rolling stock with zero-emission vehicles [1, 2]. The remainder of the article contains a proposal for installing a hydrogen drive on a three-carriage electric multiple unit. Related analyses involved two variants concerned with the vehicle power and maximum speed.

Fig. 1. Three-carriage electric multiple unit

2. Test object

The simulation involved a three-carriage electric multiple unit with two driving bogies located in the outermost carriages. Calculations were performed using generally accepted formulas for motion resistance and the adhesion curve [3, 4, and 5]. The vehicle parameters required for the performance of simulations are presented in Table 1.

The electric power required for traction purposes and own needs was limited by the momentary power of the bidirectional DC/DC 750 V/3000 V converters and the discharging and charging power of the battery. In variant no. 1, the electric power for traction purposes and own needs amounted to 2 × 375 kW = 750 kW, whereas in variant no. 2, the power was increased to 3 × 375 kW = 1125 kW.

Table 1. Vehicle parameters required for simulations

Parameter	Variant 1	Variant 2
Vehicle weight without passengers	150000 kg	150000 kg
Vehicle weight with passengers	180000 kg	180000 kg
Number of carriages	3	3
Number of drive wheelsets	4	4
Number of rolling wheelsets	8	8
Traction gear efficiency	0.98	0.98
Efficiency of traction motors	0.93	0.93
Efficiency of inverters	0.98	0.98
Rotating mass coefficient	1.07	1.07
Estimated own needs	64.61 kW	64.61 kW
Battery storage capacity	2 × 150 kWh	2 × 150 kWh
Charging and discharging power	2 × 375 kW	3 × 375 kW
Momentary power of DCDC converters	2 × 375 kW	3 × 375 kW
Electric power of hydrogen fuel cells	2 × 200 kW	3 × 200 kW

3. Traction characteristics

The traction characteristics of the vehicle against the background of the motion resistance curves are presented in Figures 2 and 3. The first characteristic was developed for an electric power source having a power of 2 × 375 kW, whereas the second characteristic was developed for an electric power source having a power of 3 × 375 kW.

As regards the achievement of the previously set traction parameters, the power of electric traction motors was a key parameter of the vehicle. Taking into account the vehicle

mgr inż. Patryk Radziszewski, dr inż. Maksymilian Cierniewski, mgr inż. Karol Bryk – Sieć Badawcza Łukasiewicz – Łukasiewicz Research Network – Poznań Institute of Technology, Centre for Modern Mobility, Poland / Poznański Instytut Technologiczny, Centrum Nowoczesnej Mobilności, Polska

Corresponding Author: patryk.radziszewski@pit.lukasiewicz.gov.pl

own needs and losses resulting from the efficiency of traction inverters, traction gears and traction motors, the obtainable mechanical power at the wheels amounted to 617 kW in relation to variant 1 and 956 kW in relation to variant 2. Figure 2 presents the traction characteristics against the background of the vehicle motion resistance curves in relation to variant 1. The vehicle was characterised by sufficient power to reach a maximum speed of 90 km/h on a straight track. On a 10 ‰ inclination, the maximum speed dropped to 84 km/h. In turn, on a 20 ‰ inclination, the maximum speed dropped to 54 km/h. Figure 3 presents the traction characteristics against the background of the vehicle motion resistance curves in relation to variant 2. The vehicle was characterised by sufficient power to reach a maximum speed of 120 [km/h] on a straight track. On a 10 ‰ inclination, the maximum speed dropped to 113 km/h. In turn, on a 20 ‰ inclination, the maximum speed dropped to 78 km/h.

4. Demand for energy

The tests involved a series of theoretical vehicle rides on the Łódź Widzew – Skierniewice and Skierniewice – Łódź Widzew routes. The assumed stop time for each stop between the initial and terminal stations amounted to 30 s.

The traction characteristics were used to calculate energy consumption for individual rides (Table 3). The rides from Łódź Widzew station towards Skierniewice performed at a maximum speed of 90 km/h were characterised by energy balance in the traction energy storage, regardless of the number of stops at intermediate stations. Such a situation resulted from a relatively significant altitude difference between the stations. The return ride required climbing a positive route profile, resulting in higher energy consumption and partial undercharging of the energy storage at the end of the route. The partial discharge of the traction battery at the end of the route did not undermine

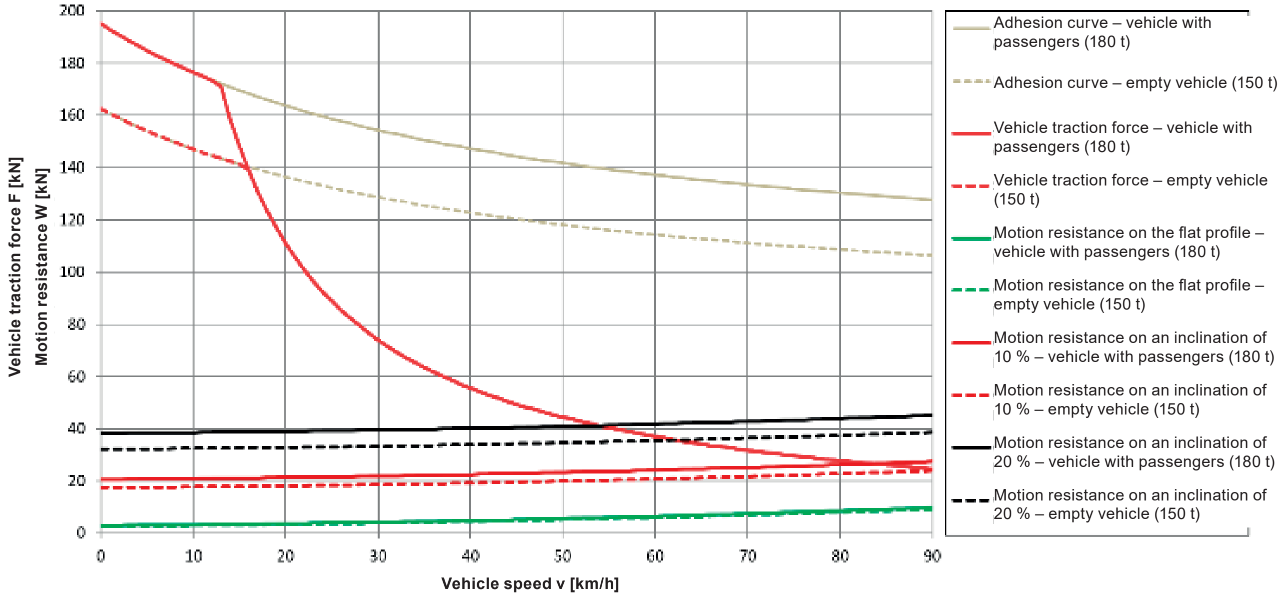

Fig. 2. Traction characteristics of a vehicle having a power of 750 [kW], vehicle mechanical power of 617 [kW]

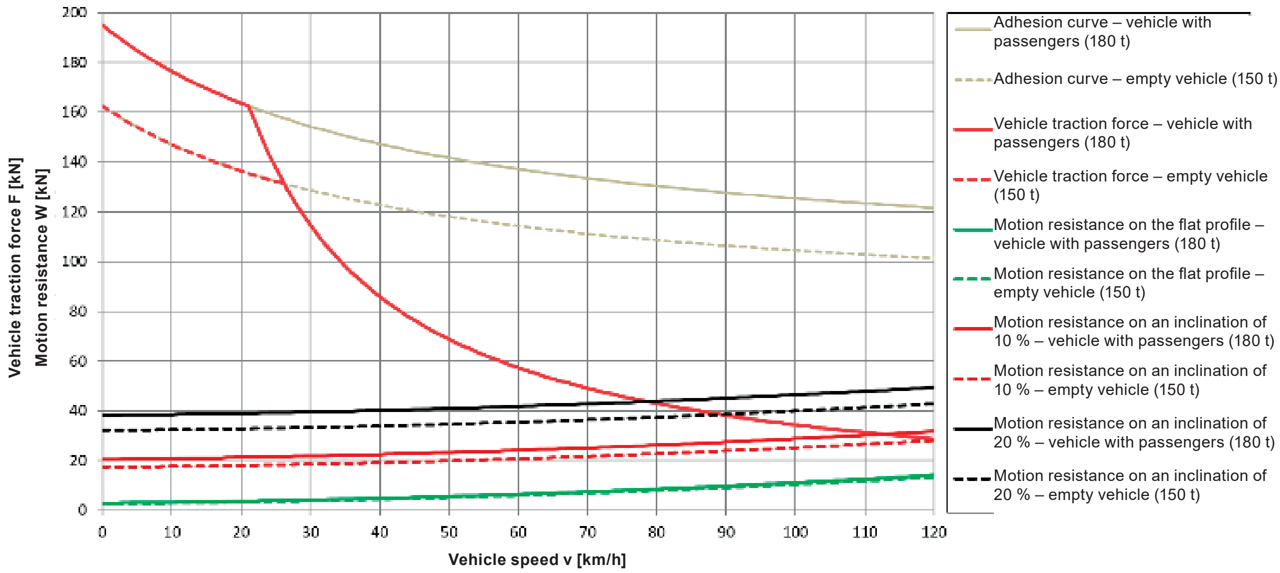

Fig. 3. Traction characteristics of a vehicle having a power of 1125 [kW], vehicle mechanical power of 956 [kW]

Table 2. Theoretical rides

Ride no.	Variant	Direction	Route length [km]	V_{max}	Number of stops
1	1	Łódź – Sk.	60.487	90	3
2	1	Sk.– Łódź	59.597	90	3
3	1	Łódź – Sk.	60.487	90	14
4	1	Sk.– Łódź	59.597	90	14
5	1	Łódź – Sk.	60.487	120	3
6	1	Sk.– Łódź	59.597	120	3
7	1	Łódź – Sk.	60.487	120	14
8	1	Sk.– Łódź	59.597	120	14
9	2	Łódź – Sk.	60.487	90	3
10	2	Sk.– Łódź	59.597	90	3
11	2	Łódź – Sk.	60.487	90	14
12	2	Sk.– Łódź	59.597	90	14
13	2	Łódź – Sk.	60.487	120	3
14	2	Sk.– Łódź	59.597	120	3
15	2	Łódź – Sk.	60.487	120	14
16	2	Sk – Łódź	59.597	120	14

Table 3. Consumption of energy

Ride no.	Variant	Energy generated in FC [kWh]	Energy at the end of the ride [kWh]	Battery discharge status [%]	Total consumption [kWh]
1	1	230.87	300.00	0	230.87
2	1	286.77	254.48	15.17	332.30
3	1	333.61	300.00	0	333.61
4	1	361.75	228.72	23.76	433.03
5	1	231.96	243.78	18.74	288.18
6	1	244.33	156.50	47.83	387.82
7	1	326.31	243.30	18.90	383.02
8	1	352.24	194.40	35.20	457.86
9	2	237.11	300.00	0	237.11
10	2	359.11	300.00	0	359.11
11	2	381.58	300.00	0	381.58
12	2	438.04	300.00	0	438.04
13	2	302.74	300.00	0	302.74
14	2	328.52	227.91	24.03	400.62
15	2	380.91	300.00	0	380.91
16	2	448.17	274.09	8.64	474.08

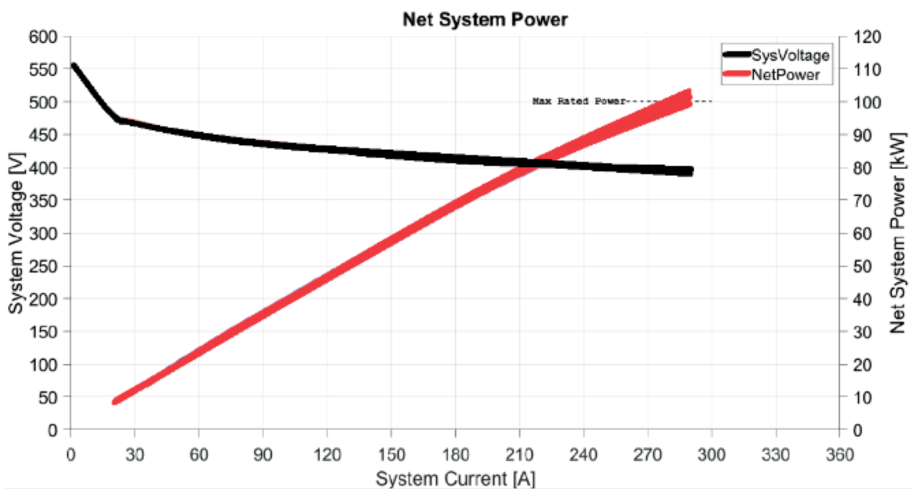

Rys. 4. Charakterystyka mocy ogniwa wodorowego

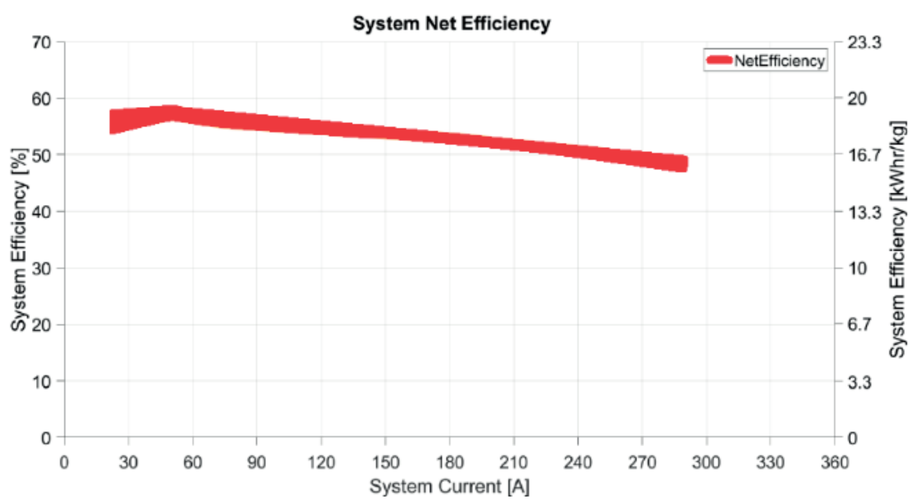

Rys. 5. Charakterystyka wydajności ogniwa wodorowego

Table 4. Hydrogen consumption

Ride no.	Hydrogen (H2) consumed [kg]	Fuel cell (FC) efficiency [kWh/kg]	Hydrogen (H2) consumed [kg]	Average consumption [kg/100 km]	Average consumption [kg/100 km]
1	17.14	13.47	39.19	32.64	38.50
2	22.05	13.00			
3	25.48	13.09	53.28	44.36	
4	27.80	13.01			
5	17.83	13.01	36.62	30.50	36.95
6	18.79	13.01			
7	25.07	13.02	52.13	43.41	
8	27.07	13.01			
9	16.38	14.47	43.24	36.01	43.70
10	26.86	13.37			
11	28.64	13.32	61.72	51.40	
12	33.08	13.24			
13	22.91	13.21	48.16	40.10	46.23
14	25.25	13.01			
15	28.48	13.38	62.88	52.36	
16	34.40	13.03			

the appropriateness of the selection of the storage capacity and the power of the hydrogen fuel cells. During the stop, the vehicle could be charged from the working fuel cell or the workshop power supply.

The consumption of hydrogen was calculated using the theoretical characteristics of hydrogen fuel cells. For simulation-related purposes, it was assumed that the full power of the fuel cells would be used for traction purposes and for charging the energy storage. In order to minimise hydrogen consumption in terms of the actual vehicle, the control system should take into account the fuel cell efficiency curve.

The performance characteristics of the hydrogen fuel cell were used to estimate the hydrogen consumption in individual rides (Table 4).

For the purposes of simulation, due to the capacity of the traction battery and in order to provide full power for the traction motors, the hydrogen cells operated close to their maximum power. According to the available data, the fuel cell efficiency in the above-presented case amounted to approximately 13 kWh/kg of hydrogen consumed. In variant 1, in relation to rides at speeds of 90 km/h and 120 km/h and a small number of intermediate stations (rides 1, 2, 5 and 6), the estimated hydrogen

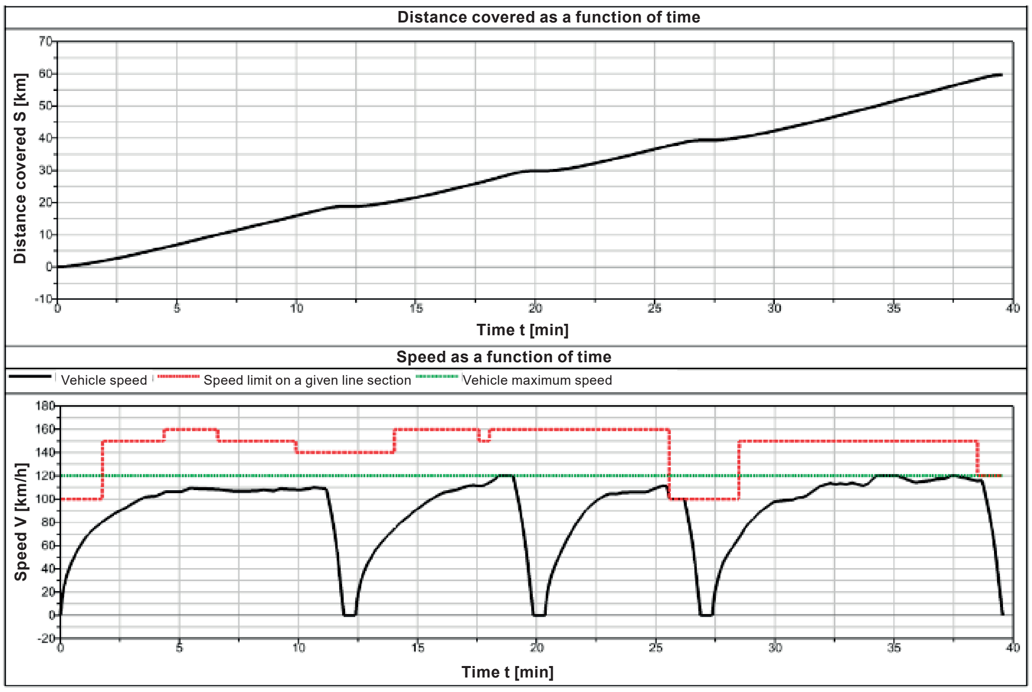

Fig. 6. Ride no. 6 – speed as a function of time

consumption amounted to 32.64 kg and 30.50 kg respectively. In cases of rides 3, 4, 7 and 8, where it was necessary to accelerate the vehicle numerous times, the consumption increased to 44.36 kg in relation to a speed of 90 km/h and to 43.41 kg in relation to a speed of 120 km/h. Lower hydrogen consumption during the rides with a previously assumed maximum speed of 120 km/h was directly connected with the smaller amount of energy remaining in the traction energy storage.

In variant 2, in relation to rides at speeds of 90 km/h and 120 km/h and a small number of intermediate stations (rides 9, 10, 13 and 14), the estimated hydrogen consumption amounted to 36.01 kg and 40.10 kg respectively. In cases of rides 11, 12, 15 and 16, where it was necessary to accelerate the vehicle many times, the consumption increased to 51.40 kg in relation to a speed of 90 km/h and to 52.36 kg in relation to a speed of 120 km/h.

5. Theoretical rides

The diagrams of theoretical rides enabled the comparison of the appropriateness of selected drive parameters in relation to the vehicle route, vehicle permitted maximum

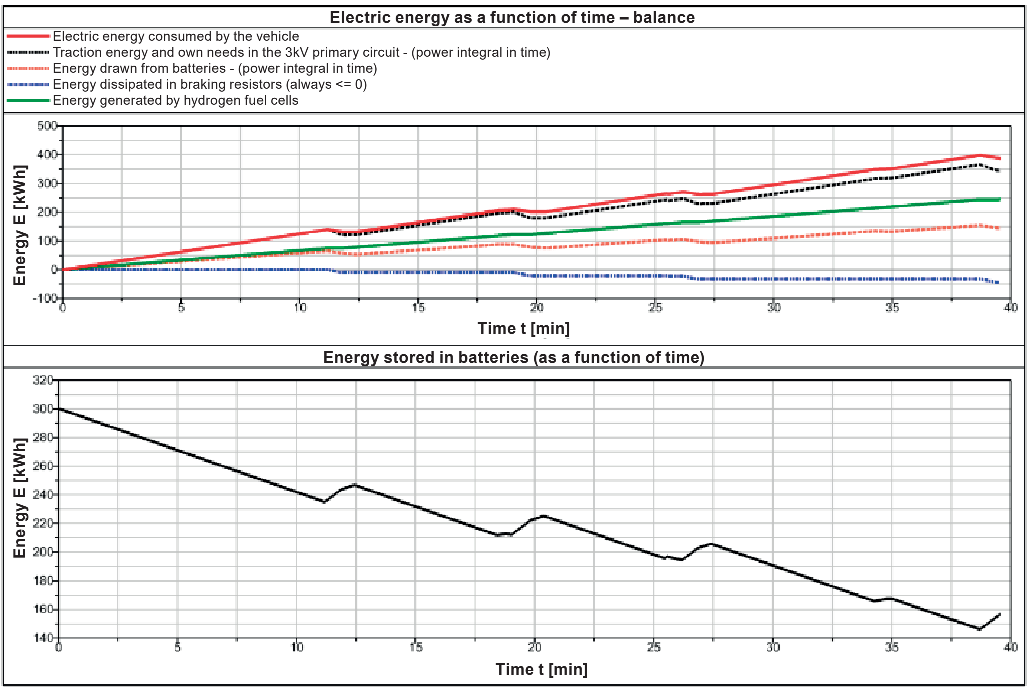

Fig. 7. Ride no. 6 – energy consumption as a function of time

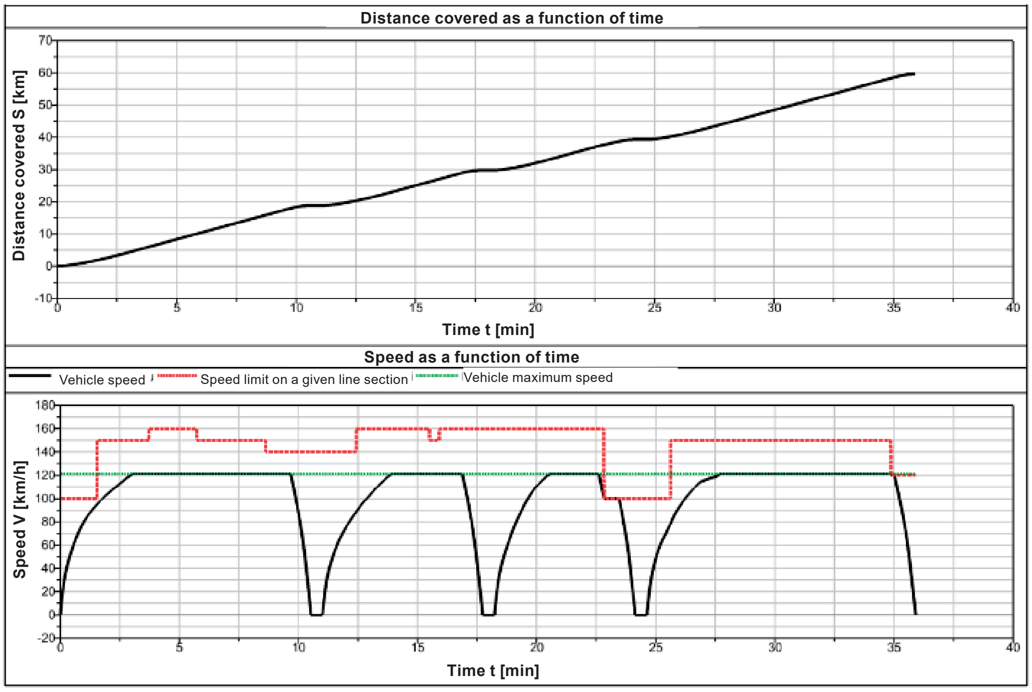

Fig. 8. Ride no. 14 – speed as a function of time

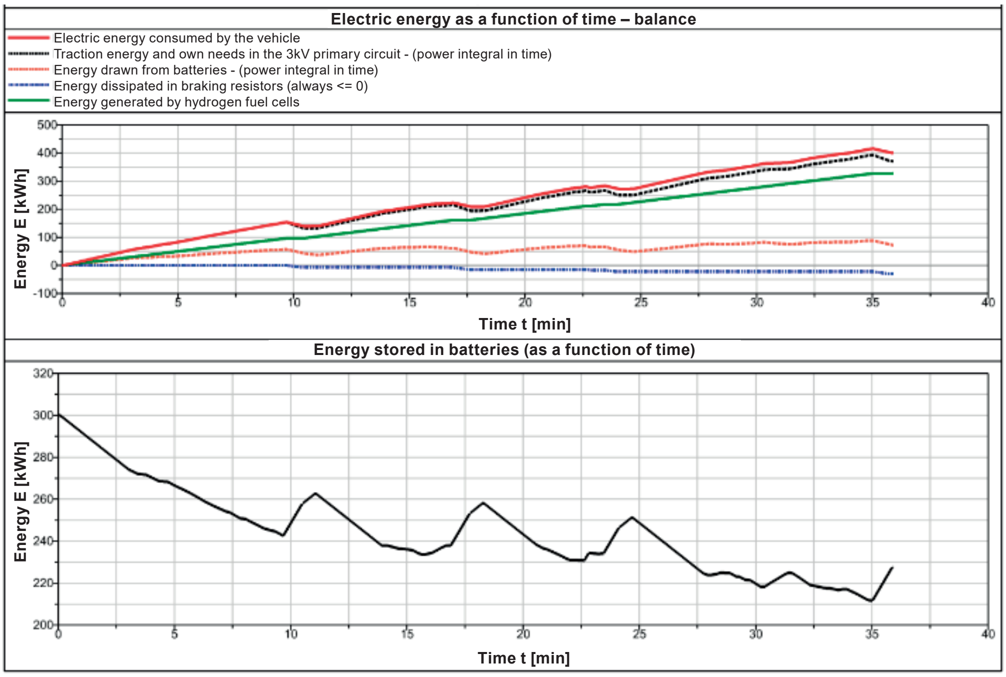

Fig. 9. Ride no. 14 – energy consumption as a function of time

speed and the number of stops. Presented below are analogous rides in relation to a vehicle having a power of 750 kWh (Fig. 6 and Fig. 7) and a vehicle having a power of 1125 kWh (Fig. 8 and Fig. 9).

In terms of the ride with a positive route inclination (Fig. 6), the vehicle reached a maximum speed only on some sections of the route.

Traction storage discharge diagram. The calculated energy remaining in the storage after the end of the course amounted to 156.50 kWh. In relation to the maximum energy of 300 kWh, the discharge stood at 47.83 %.

Figure 8 presents the ride with a positive route inclination. The vehicle reached the maximum speed along most of the route.

Traction storage discharge diagram. The calculated energy remaining in the storage after the end of the course amounted to 227.91 kWh. In relation to the maximum energy of 300 kWh, the discharge stood at 24.03 %.

6. Summary

The results were characterised by a significant difference in energy consumption in relation to the direction of the ride, which, in turn, resulted from a relatively significant altitude difference between Łódź Widzew station and Skierniewice station. In variant 2, the vehicle consumed up to 15 % more energy (Table 3) than in variant 1. However, it should be noted that greater traction power enabled the vehicle to reach the previously set maximum speed in a shorter time, which was of great importance in terms of meeting the timetable. In variant 1, the vehicle was characterised by the greater use of the energy buffer (i.e. the traction storage). The partial discharge of the traction battery at the end of the route did not undermine the appropriateness of the selection of the storage capacity and the power of the hydrogen fuel cells. During the stop, the vehicle could be charged from the working fuel cell or the workshop power supply.

REFERENCES

[1] Durzyński Z., Hydrogen-powered drives of the rail vehicles (part 1), Rail Vehicles/Pojazdy Szynowe, 2021, no. 2, pp. 29–40, ISSN 0138-0370.
[2] Durzyński Z., Hydrogen-powered drives of the rail vehicles (part 1), Rail Vehicles/Pojazdy Szynowe, 2021, no. 3, pp. 1–11, ISSN 0138-0370.
[3] Karwowski K., Energetyka Transportu Zelektryfikowanego, Wydawnictwo Politechniki Gdańskiej, Gdańsk 2020, ISBN 978-83-7348-800-7.
[4] Podoski J., Kacprzak J., Mysłek J., Zasady trakcji elektrycznej, WKiŁ, 1980, ISBN 83-206-0095-2.
[5] Madej J., Teoria ruchu pojazdów szynowych, Oficyna Wydawnicza Politechniki Warszawskiej, Warszawa 2012, ISBN 978-83-7207-487-4.

The article was presented at the 32nd Scientific and Technical Conference "Problems of Exploitation of Electric Machines and Drives" – PEMINE (Słok near Bełchatów, 2–4.10.2024).

Łukasiewicz Sieć Badawcza
Łukasiewicz Poznański Instytut Technologiczny

The research work discussed in the above-presented article was co-financed from the state budget – special-purpose subsidy of the President of the Łukasiewicz Centre "Complete hydrogen vehicle control system" – H2CONTROL